Chapter 4

Reversed Cyclically Loaded Dowel-Type Fasteners

4.1 General

In contrast to nailed connections, little research has been done on bolted connections using a reversed cyclic loading scheme, although cyclic loading provides important information about energy absorption and damping properties, which is essential when analyzing seismic performance. Dowrick (1986) noted that the hysteretic characteristics for the primary connection of a subassembly govern its cyclic behavior. If the hysteretic behavior of timber joints is determined, the behavior of timber structures and structural systems can be characterized (Foliente and Zacher 1994).

4.2 Cyclic Behavior of Bolted Joints

Timber joints are designed to undergo inelastic deformations during dynamic loading associated with natural disasters such as earthquakes or high winds. It would be inefficient, both in terms of amount of material used and expenses incurred, to attempt the design of structures to perform within the elastic range during high intensity cyclic loading. Excitation loads that produce inelastic deformations associated with dissipation of energy, generate a stress-strain response (which can also be mapped in the load-slip plane) which is referred to as hysteresis. Bolted joints in timber exhibit "pinched" load-slip hysteresis loops due to a progressive degradation of lateral stiffness for each successive loading cycle (Figure 4.1). The resisted load decreases between two successive cycles at the same displacement level. Cyclic stiffness degradation is a result of the fastener crushing the wood fibers surrounding it at each progressive displacement phase beyond the elastic limit. A cavity is formed around the bolt, leaving the fastener unsupported during successive cycles until the displacement increases and the fastener again becomes supported by the previously crushed timber. But, until the shank contacts the crushed timber, only bending resistance of the bolt shank within the cavity and friction counteracts the external force. This is reflected in the pinched part of the hysteresis loops. As displacement increases, more fibers crush around the bolt and the cavity enlarges. The part where the external force is resisted by bolt bending increases. Consequently the pinched sections of the hysteresis loops become longer.

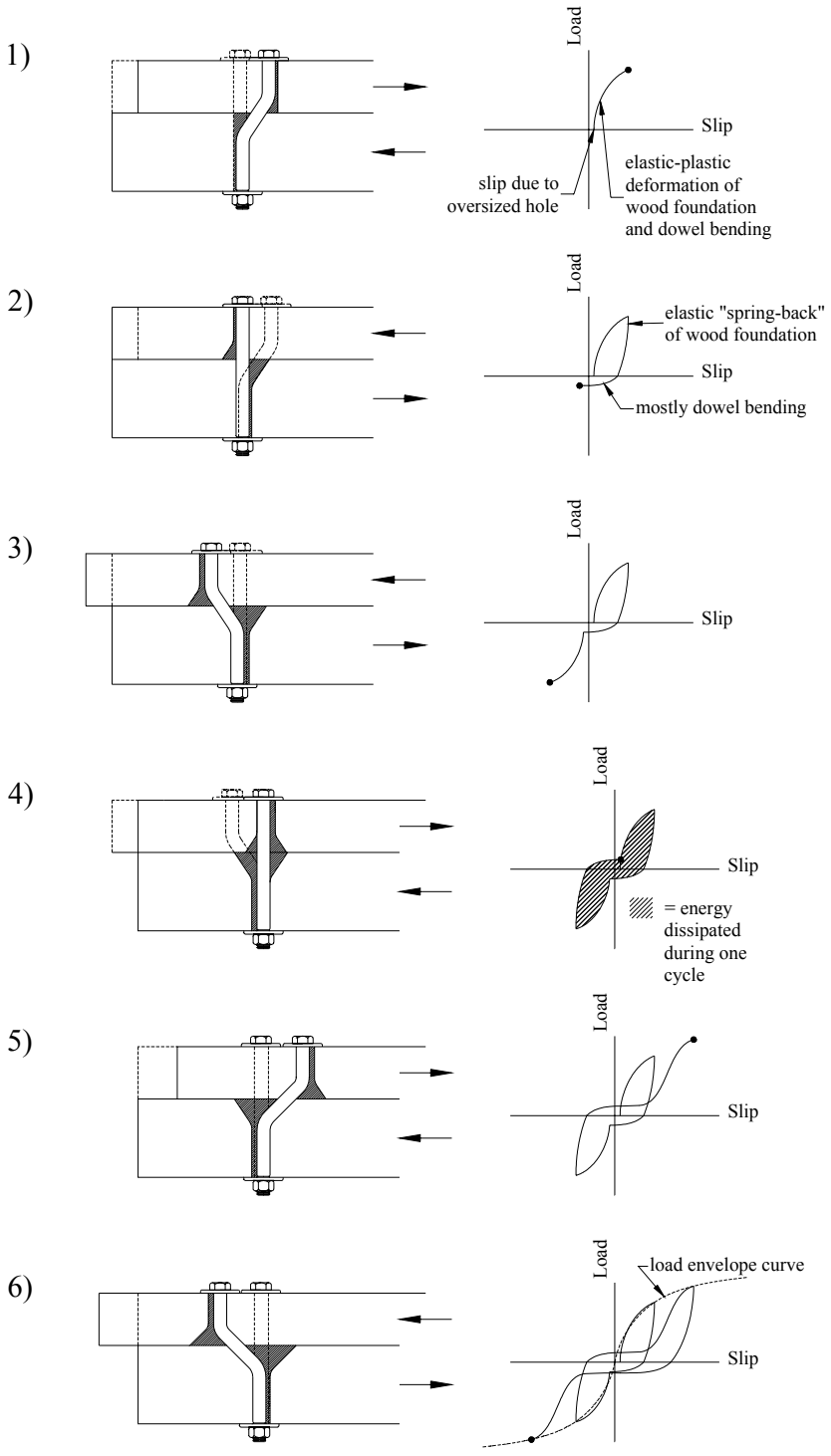

Figure 4.1: Hysteretic performance of a bolted joint in single shear stressed beyond the elastic limit. Left side shows the bolt at various deformation states. Corresponding load-slip curves are depicted on the right.

4.2.1 Effect of Cyclic Loading on Connection Properties

It is noteworthy that no commonly agreed upon guidelines for data reporting, data analysis and performance evaluation methods of cyclically tested timber joints exist to date. Although joint properties are influenced by data analysis techniques, and the definition of the properties themselves (which vary to a great extent in the literature), general observations about connection properties can be made.

European research on the seismic behavior of joints in wooden structures indicates that in most cases the cyclic envelope curve and the monotonic load slip curve almost coincide with a difference of less than 10 percent (Ceccotti 1995). Exceptions are fatigue failures and fastener pull-outs due to cyclic loading. This hypothesis is not unanimously agreed upon, however, as the following discussion reveals.

4.2.1.1 Strength

Findings reported in the literature are somewhat contradictory as to whether cyclic loading increases or decreases connection capacity of the single fastener when compared to one-directional static loading. Cruz et al. (1991) tested the reversed cyclic embedment strength (loading rate: 20mm/min) of nails and recorded an increase of embedment strength when subjected to cyclic loading. This finding was confirmed by Chui and Ni (1997) through cyclic (frequency: 0.25Hz and 0.5Hz) and monotonic embedment tests on nails. Earlier, Ni and Chui (1994) found the same trend for lateral resistance of the total joint. They observed that the lateral load resistance was substantially higher for joints loaded cyclically (frequency: 1Hz and 3Hz) than for statically stressed joints. However, Dolan et al. (1996) noted a significant decrease in ultimate lateral resistance of bolted joints under load reversal (frequency: 1Hz). Yasumura (1998) reported similar observations. Joint capacity of bolted joints with steel side plates subjected to reversed cyclic loading (loading rate: 0.2mm/sec) was reduced up to 40 percent when compared with one-directional loading. Yet, Yasumura could not observe a significant reduction of strength for dowel joints with a steel center plate. Considering these findings it is not clear whether material differences, fastener diameter, and/or loading rates and procedures can be attributed to the presented discrepancies.

As opposed to the effect of load reversal on capacity, it is well established that resistance degrades when a joint is repeatedly loaded up to the same displacement level. Lateral load of bolted connections reduces up to 26 percent when the connection is displaced to a given displacement multiple times (Dolan et. al 1994). Generally, after four cycles at constant

displacement level, strength degradation diminishes and stabilized connection response is attained (Daneff et al. 1996).

In the case of cyclic loading of multiple-bolt joints, there may be an increase in capacity when compared to monotonic loading, partly due to load redistribution (Mohammad et. al 1998). However, at the present state of knowledge, the amount of studies conducted to investigate the response to reversed cyclic loading of more than one fastener in a row is disturbingly small.

4.2.1.2 Stiffness

Wilkinson (1976) published data from vibrational tests on nailed and bolted wood-to-wood connections and induced that initial stiffness increases significantly under cyclic loading. Research carried out in Canada on multiple bolted connections substantiated Wilkinson's results (Mohammad et. al 1998). But between successive loading cycles and at increasing displacements, lateral stiffness degrades, which is attributed to hysteretic pinching (Dolan et. al 1994). Cycling beyond the elastic limit introduces slackness to the joint due to a cavity that forms around the fastener shank. It is believed that slackness increases the natural period of oscillation (Dean et al. 1986). It is further believed that joint slackness leads to a force reduction and isolates the mass of timber structures from high ground acceleration peaks during earthquakes (Deam and King 1994). Slackness is one of the main reasons why timber structures have performed satisfactory during earthquakes although energy dissipation is far less compared to steel structures, which is attributed to the pinched hysteresis loops.

4.2.1.3 Ductility

Bolted joints subjected to reversed cyclic loading reach capacity at considerably lower slip than joints loaded monotonically (Daneff et al. 1996; Dolan et. al 1994). Similar observations were made during reversed cyclic tests of wooden subassemblies such as shear walls (Heine 1997, Johnson 1997).

4.2.2 Rate of Loading Effects

Chui and Ni (1997) noted that ultimate embedment strength of nails subjected to several loading frequencies increases with increasing frequency (or loading rate). In addition, the researchers indicated that initial stiffness of the envelope curve is positively correlated with loading rate. On the other hand, Girhammer and Anderson (1988) could not find a significant difference among data of elastic stiffness of laterally loaded nail joints under various monotonic loading rates, but they did acknowledge a logarithmic increase in capacity with higher loading rate.

With the information available today, it is safe to assume that the true behavior of joints in wood structures subjected to instantaneous loading as is typical in earthquakes would be characterized by higher stiffness and higher lateral strength than observed during periodic cyclic laboratory tests (Ceccotti 1995).

4.3 Modeling of Connections under Cyclic Load

All of the wood and non-wood parts of the connection, and the interaction of those parts, dictate the static strength of a connection. All of the factors that affect static connection performance presumably affect the cyclic performance as well. But the reverse is not true. Not all factors that influence cyclic behavior have an effect on static performance. This is why the study of cyclic/dynamic loading is so important. There exists a substantial body of literature covering the quasi-static monotonic strength of dowel-type connections (see McLain and Thangjitham 1983). Yet under reversed cyclic loading, connection strength and stiffness are related to load history. That is, the load-slip relation of each loading cycle is influenced by the load magnitude of the preceding cycle. It is this load history (or memory) effect that makes modeling of timber joints under cyclic loading considerably more complex than the formulation of a unidirectional load-displacement model. Due to memory, it is not possible to simply apply existing methods used to model static behavior of joints for connections subjected to cyclic excitations. Moreover, conventional models used to approximate the elastic-plastic behavior of steel and concrete are not applicable for timber structures, as they do not allow for incorporation of slackness or pinching (Deam 1994).

The core of any analytical model attempting to describe the response of cyclically loaded timber connections is the formulation or method that describes the hysteresis. Apart from the hysteretic model, the same analytical tools may be used as for static analysis. Thus, the following section will discuss major hysteresis formulations that have been advanced by several researchers.

4.3.1 Hysteresis Modeling

Not all models discussed below were formulated for timber connections in particular. Instead several hysteresis models were developed to replicate the cyclic response of timber structures such as shear walls or entire buildings. However, it is well established that the behavior of timber structures is governed by the load slip characteristic of the primary connection (Foliente 1994; Dowrick 1986; Steward 1987; Dolan 1989; Yeh et al. 1971). Therefore, most models that were intended to model an entire structure could be applied to connections as well

with little modification. The most widely used hysteresis formulations are those that in one way or another follow a "set of rules" that specify stiffness functions and transition points for various cases such as loading, unloading, loading after previous loading, etc.

In an effort to model numerically the cyclic behavior of shearwalls, Stewart (1987) advanced a hysteretic approximation consisting of a series of straight-line segments (Figure 4.2). Hysteretic force follows the initial stiffness, k_0, until a predefined 'yield point' is reached. Stiffness is reduced by a bilinear and trilinear factor r_1 and then r_2 depending on when unloading occurs. The "pinching stiffness", k_p, is expressed in terms of the initial stiffness according to

$$k_p = k_0 \left(\frac{\Delta_{yield}}{\Delta_{un}} \right)^{\alpha} \tag{4.1}$$

where,

$$\Delta_{un} = \beta \cdot \Delta_{\max} \tag{4.2}$$

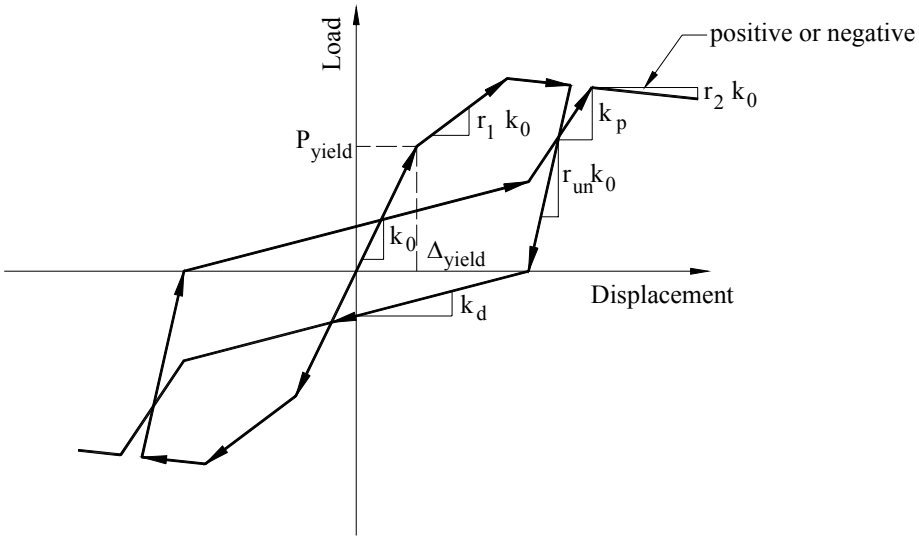

Figure 4.2: Hysteresis model as utilized by Stewart (1987)

		Unit
k_0	initial wall stiffness	N/m
k_p	pinching stiffness	N/m
k_d	degrading stiffness	N/m
k_1	bilinear wall stiffness	N/m
k_2	trilinear wall stiffness	N/m
α	parameter controlling rate of stiffness degradation	
β	"softening parameter"	
Δ_{yieldx}	yield displacement as defined in	m
Δ_{un}	wall displacement where unloading occurs	m
Δ_{max}	preceding maximum displacement in the respective loading direction	m
r_1, r_2, r_{un},	stiffness parameters	

Steward used "a step-by-step numerical integration technique" to solve the model.

Dolan (1989) developed two hysteresis formulations as part of a finite element program that numerically analyses the cyclic response of timber framed shear walls with plywood or waferboard sheathing. The first model is a relatively simple bilinear model that approximates the hysteresis of a shear wall using six linear segments. This model was employed to investigate the steady state frequency response function for the entire wall structure. Through the obtained frequency response spectrum, it could be observed that nailed shear walls exhibit stable response at constant excitation amplitude and frequency. Dolan modeled the wall as a single degree of freedom system consisting of mass and spring with hysteretic characteristics allowing the omission of a viscous damper. The envelope curve was assumed to follow Equation (2.21). The hysteresis formulation is based on the estimation of four parameters, which Dolan obtained through least-square curve fitting using data acquired from cyclic tests on full-scale walls (Figure 4.3).

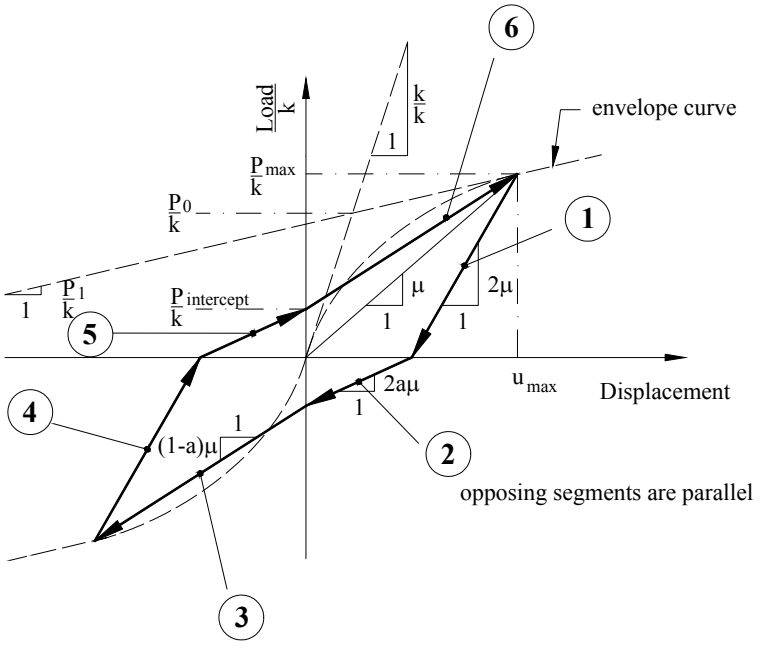

Figure 4.3: Idealized hysteresis of a timber shear wall by Dolan (1989)

Since stud-to-sheathing fasteners may experience random excitation and are the major source of energy dissipation of a shear wall structure during earthquakes, Dolan developed a second hysteresis model that described the response of an individual sheathing nail (Figure 4.4). Based on the information gathered by the shear wall model, the fastener model is a more sophisticated hysteresis model that more closely approximates the true hysteretic behavior using four exponential equations. The model was solved numerically.

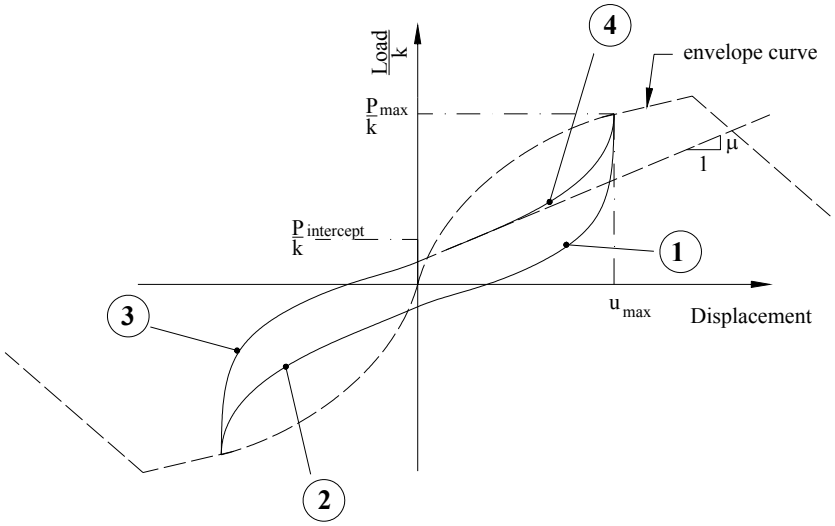

Figure 4.4: Modeled hysteresis behavior of sheathing connector element by Dolan (1989)

		Unit
k	initial wall stiffness	N/m
a	ratio of peak hysteretic load to load at intercept	
μ	slope of line passing through origin and peak hysteretic load in	
P_0	slope of asymptote	N/m
P_{max}	peak hysteretic load per cycle	N
$P_{intercept}$	hysteretic load at zero displacement	N
u_{max}	maximum hysteretic displacement per cycle	m

Many models replicate the response of the entire connection making them case dependent, which means that each new joint configuration has to be tested first to obtain the necessary input parameters. In contrast to statically stressed connections, very little research has been conducted to determine the cyclic response of the individual components of a joint, such as the cyclic embedment behavior of wood. Little, if any, experimental studies have been done to relate cyclic embedment strength to specific gravity and fastener diameter. Based on substantially different behavior of wood under cyclic loading, it is reasonable to question whether Equations 2.2 and 2.3 derived by Wilkinson (1991) are valid for cyclic loading. To close the discrepancies between the knowledge of static and cyclic behavior, a "component approach" to modeling cyclic structures should be striven for, where ultimately input variables constitute basic material properties.

The modeling approach of Chui et al. (1998) was an attempt towards the component approach. The researchers presented a versatile nonlinear finite element model whose input consists of basic mechanical properties. The model predicts the cyclic response of a nailed timber joint in single shear. The hysteretic formulation was broken down into a hysteretic embedment model of wood and a separate stress-strain model describing the nail material (Figure 4.5). For the fastener material, the researchers adopted a hysteretic model put forth by Filippou et al. (1983).

The embedment envelope curve depicted in Figure 4.5 b) is a modification of Equation (2.21) to include the effect of strength degradation beyond capacity. When subjected to monotonic loading, wood hardly exhibits strength degradation during embedment tests of small diameter fasteners where premature splitting does not occur (Chui and Ni 1997). Strength degradation was modeled by a second asymptote with stiffness k_2.

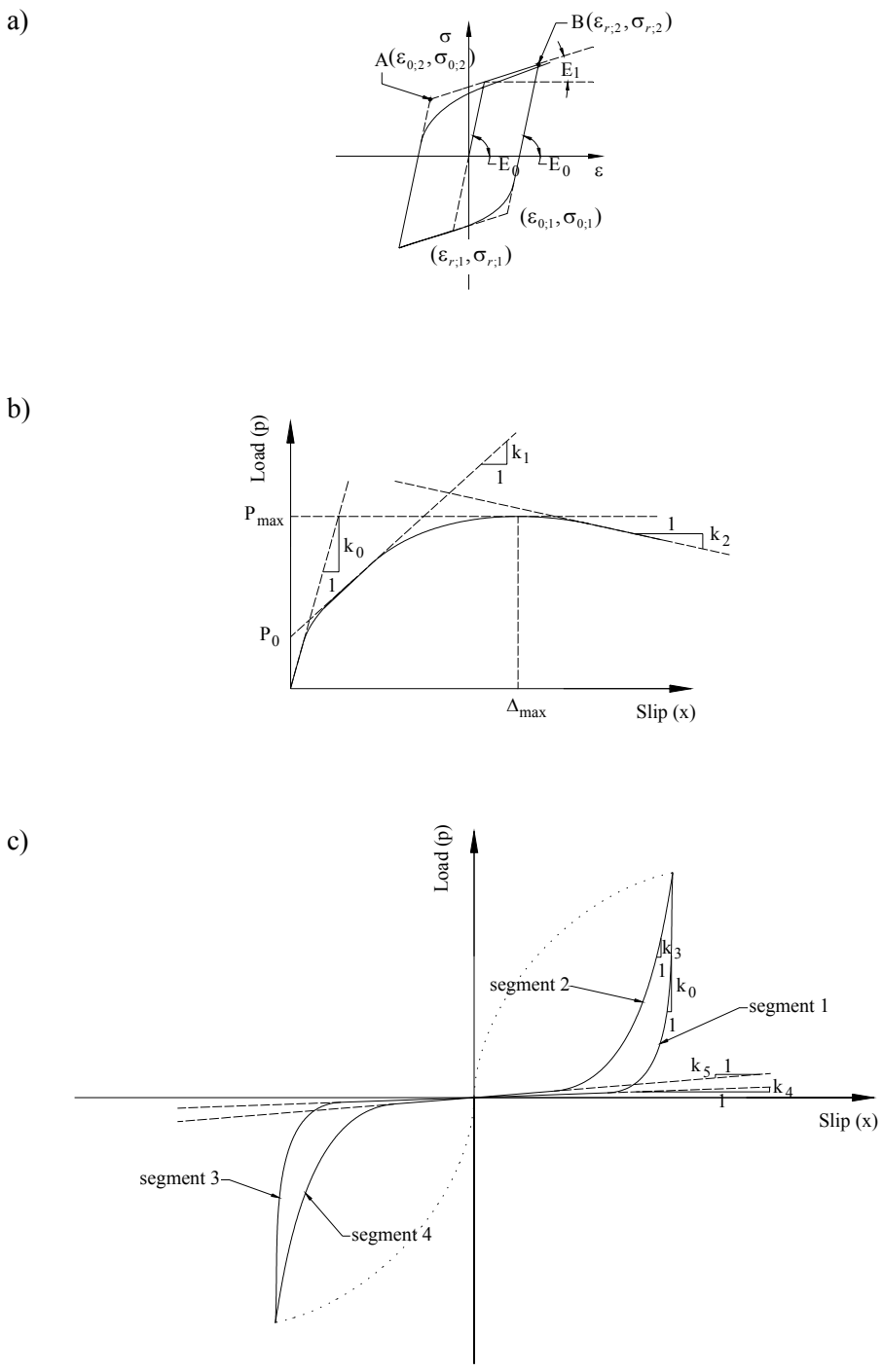

Figure 4.5: a) Stress – strain model for a single nail b) Modeled envelope curve c) Hysteresis model representing the embedment behavior of wood by Chui et al. (1998).

The embedment hysteresis model (Figure 4.5 c) is of similar structure as the fastener model proposed earlier by Dolan (1989). However, the hysteretic force is determined by a different set of equations since fastener bending and yielding are not included. For more detailed information, the reader is referred to Chui and Ni (1997). In contrast to Dolan's model, during unloading, the embedment load approaches zero first rapidly and then along a straight lined path with close to zero stiffness, k_4, as more and more wood gets crushed. The parameters shown in Figure 4.5 c) (maximum displacements and the corresponding hysteretic loads) define the path of each segment. The model was solved iteratively.

Other models have been advanced as part of comprehensive finite element analyses (Ceccotti and Vignoli 1990, Foschi 1993, Lee 1987, Komatsu et al. 1988; White and Dolan 1995, Tarabia and Itani 1994). In the last thirty years the finite element analysis gained popularity and has become, thanks to improving computer technology, a useful tool to model almost any type of structural problem. Finite element analyses that were carried out in the past, usually investigated the influence of one design variable on the overall joint strength. Most formulations were limited to two-dimensional analyses investigating a maximum of two bolts in a row and elastic materials were frequently assumed. The author is not aware of any finite element formulation that predicts the behavior of a generic multiple-bolt joint (i.e. not tied to a particular species or arrangement and with oversized holes) subjected to reversed cyclic and / or dynamic excitation. Even with today's computing power available, an accurate finite element analysis of multiple bolted timber joints under cyclic loading would still require substantial resources.

Apart from hysteresis models designed to be solved in a numerical, stepwise manner, mathematical solutions are rare. The above models are not general in the sense that the solution depends on a set of programmed cases that are executed using 'IF – THEN – ELSE' statements, which makes modeling computationally inefficient if random input functions such as earthquake records are used.

Dean et al. (1986) approximated hysteretic pinching of single-degree-of-freedom structures vibrating at large displacements using the simple abstraction of a mass oscillating between two springs (Figure 4.6). However, this approximation assumes no increase in slack at growing displacements. Moreover, as was observed during tests, the resisted load does not drop to zero even in structures with significant slack development.

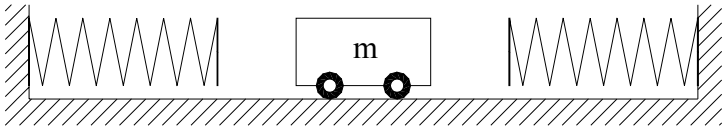

Figure 4.6: Pinching modeled by a mass oscillating between two springs (after Dean et al. 1986)

One of the first truly mathematically closed-form hysteresis models for structures was put forth by Bouc (1967) and further modified and improved by Wen (1980), Baber and Wen (1981), and Baber and Noori (1985, 1986) (BWBN model). Foliente (1993) slightly altered the pinching function of the model and tested its applicability to wood structures. He presented an excellent and very detailed discussion of the BWBN model. The BWBN model constitutes the basis for the hysteresis model developed in Chapter 5 and is introduced next.

4.3.1.1 The Bouc-Wen-Baber-Noori (BWBN) Model

The BWBN model relies on a "black-box approach", in that the complex mechanics involved in any structure that is stressed beyond the elastic limit, and that exhibits hysteretic behavior, are by and large disregarded. Instead, the modeled object is simplified and represented by an equivalent system consisting of a mass connected parallel to a linear spring, a linear viscous damper and a hysteretic element (Figure 4.7). The properties of the elements of the simplified structure are empirically adjusted to fit the problem at hand. In spite of this, the BWBN model is not to be mistaken as purely empirical. Empirical models have the disadvantage that extrapolation to cases outside the studied bounds is usually not valid. Using physical entities such as damper, spring and mass, the BWBN model, on the other hand, is valid for a wide range of input functions.

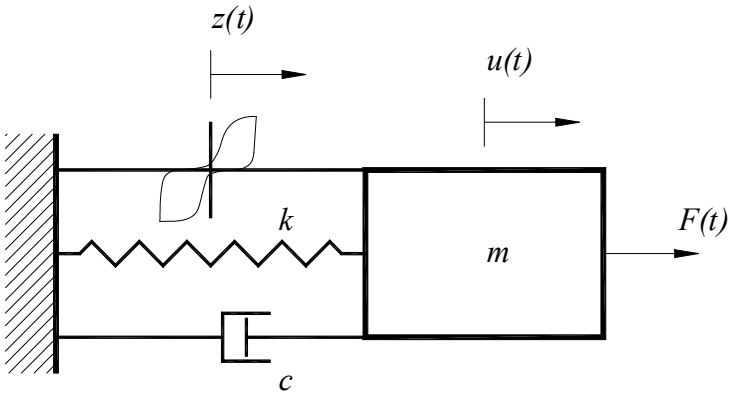

Figure 4.7: Abstract form of a hysteretic single degree of freedom system (Baber and Noori (1985))

The BWBN Model separates nonlinear and linear components. All nonlinear behavior is embodied in the hysteretic element, which is akin to a nonlinear spring. The hysteretic force is caused by a different fictitious hysteretic displacement, z, which is a function of the total displacement, u. The total energy absorbed by the hysteretic element and the hysteretic displacement control the nonlinear response. In standard form, the equation of motion is formulated as

$$\ddot{u}(t) + 2 \cdot \xi_0 \cdot \omega \cdot \dot{u}(t) + \alpha \cdot \omega^2 \cdot u(t) + (1-\alpha) \cdot \omega^2 \cdot z(t) = f(t) \tag{4.3}$$

where (Figure 4.8)

$$\alpha = \frac{k_f}{k_i} \quad \text{for} \quad 0 \le \alpha \le 1 \tag{4.4}$$

$$\dot{z} = h(z) \cdot \left[\frac{A \cdot \dot{u}(t) - \nu \cdot \left(\beta \cdot |\dot{u}(t)| \cdot |z(t)|^{n-1} \cdot z(t) + \gamma \cdot \dot{u}(t) \cdot |z(t)|^n \right)}{\eta} \right] \tag{4.5}$$

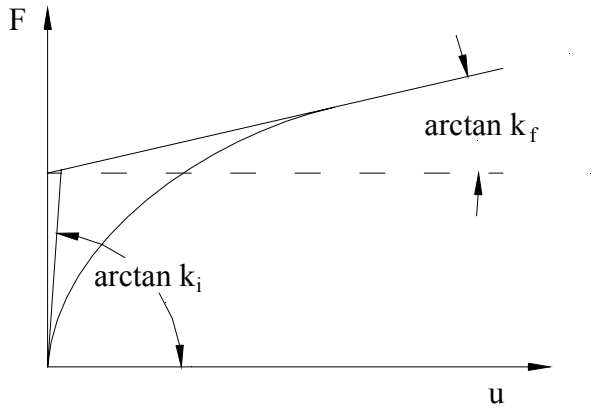

Figure 4.8: Definition of initial tangent stiffness and final stiffness

Pinching is a nonlinear function described by

$$h(z) = 1.0 - \zeta \cdot \left(1.0 - e^{(-p \cdot \varepsilon(t))}\right) \cdot e^{\left(\frac{-(z(t))^2}{\left(\left(\psi_0 + \delta_\psi \cdot \varepsilon(t)\right) \cdot \left(\lambda + \zeta \cdot \left(1.0 - e^{(-p \cdot \varepsilon(t))}\right)\right)\right)^2} \right)} \tag{4.6}$$

Response history dependency is modeled by

$$\nu(\varepsilon) = 1.0 + \delta_\nu \varepsilon(t) \tag{4.7}$$

$$A(\varepsilon) = A_0 - \delta_A \varepsilon(t) \tag{4.8}$$

$$\eta(\varepsilon) = 1.0 + \delta_\eta \varepsilon(t) \tag{4.9}$$

The absorbed hysteretic energy, ε, which controls pinching, 'strength' and stiffness degradation, is defined as

$$\varepsilon = \left(1 - \alpha\right) \cdot \omega^2 \cdot \int_{t_0}^{t_f} z(t) \cdot \dot{u}(t)\, dt \tag{4.10}$$

		Unit
ω	pseudo-natural frequency of the non-linear system	rad/sec
$f(t)$	force function (mass normalized)	N/kg
t	time	sec
ξ	viscous damping ratio	
u	total displacement of the mass, m	m
z	hysteretic displacement	m
k_i	initial stiffness	N/m
k_f	final stiffness	N/m
α	rigidity ratio	
A_0	parameter controlling hysteresis amplitude	
δ_A	parameter specifying the dependency of A to dissipated energy.	
β, γ, n	parameters describing shape and amplitude of hysteresis	
$h(z)$	pinching function; $h(z)$ = 1.0 no pinching.	
$\zeta,$	pinching parameter controlling the severity and rate of pinching	
p	parameter controlling the rate of initial drop in slope	
ψ_0	pinching parameter	
δ_ψ	parameter specifying the rate of pinching with z	
λ	pinching parameter	
ν	response history dependency; ν = 1.0 no degradation	
η	response history dependency; η = 1.0 no degradation	
δ_ν	degradation parameter.	
δ_η	degradation parameter	
ε	absorbed energy by the hysteretic element	N m/kg

Additional parameters as well as non-linear degradation may be added if deemed necessary. The term strength degradation is somewhat misleading since strength degradation can only be modeled if displacement is the input function. Subjected to a steadily increasing periodic force (Figure 4.9a), without pinching and degradation, the model describes a pointed ellipse for a certain combination of n, β and γ (Figure 4.9b). If only pinching is added, the ellipse gets pinched (Figure 4.9c). In addition, overall stiffness decreases with increasing dissipated energy, although stiffness degradation is turned off. If the input function is a periodically increasing force, then degradation simply rotates and 'stretches' the function with increasing dissipated energy (the width of the function hardly increases unlike the no-pinching, non-degradation case) (Figure 4.9d and e).

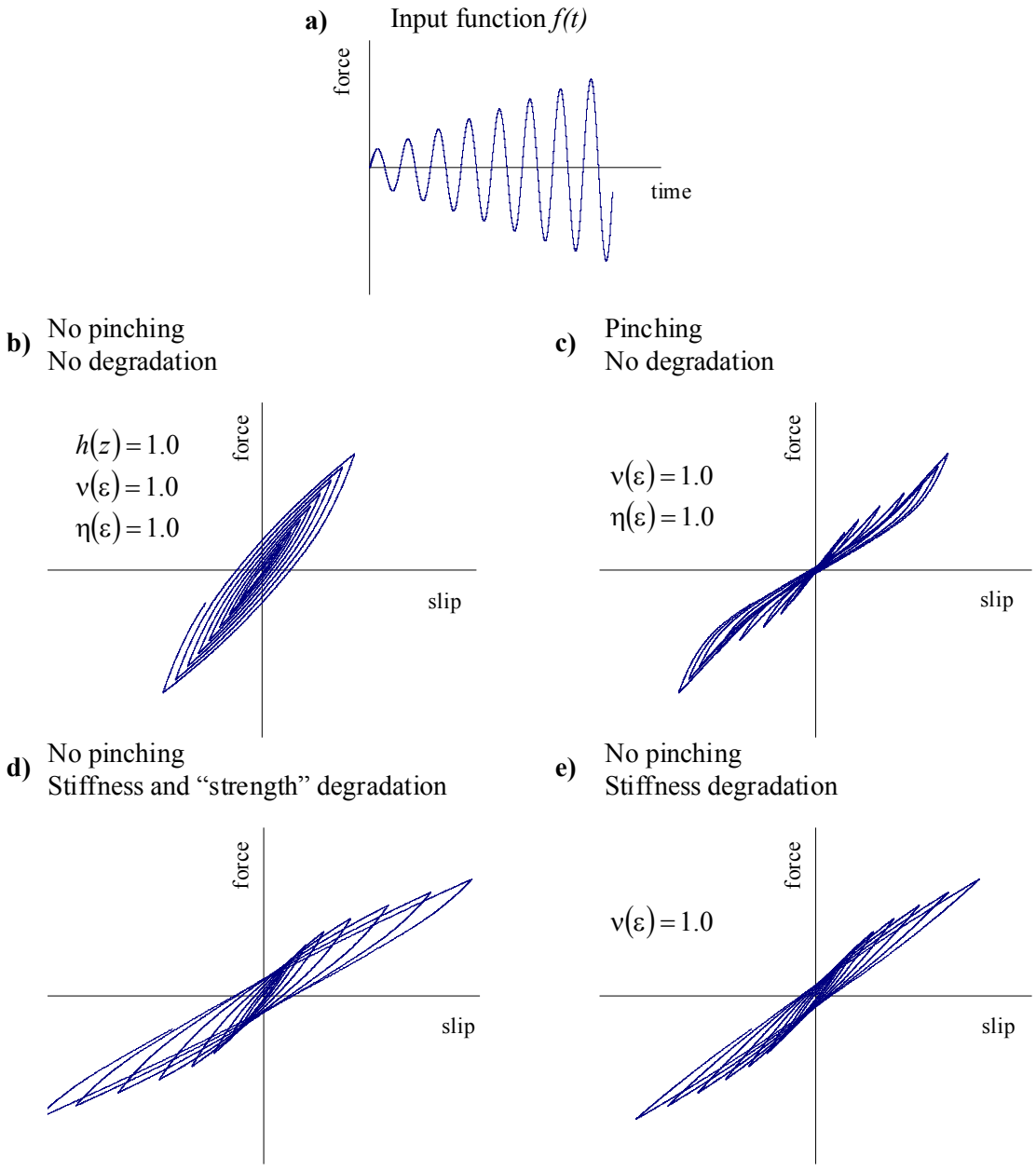

Figure 4.9: BWBN output when degradation and pinching parameters are varied. Input function is a linearly increasing periodic force.

Given that all 15 parameters are appropriately estimated, the BWBN model can be relatively easily solved with widely available software packages such as *Mathematica*, *LSODE* (see Chapter 5), or *IMSL* routines. However, especially with force as the independent variable,

the solution is extremely sensitive to some parameters and their interaction, which makes it almost impossible to correctly identify the parameters manually by trial and error.

In spite of its vast versatility and ability to produce smooth pinched hysteresis loops of various shapes, the BWBN model is not capable of tracing slack systems. At zero dissipated energy, the stiffness at the origin (initial stiffness) as modeled by BWBN always assumes maximum value. For slack systems, however, initial stiffness is zero or close to zero until the slack is overcome. In case of stiff fasteners such as bolts, this is true even if the slack is very small or approaches zero, which is evident from embedment test data published by Wilkinson (1991), Brinkman (1996), Stamato and Calil (1999), and from load-displacement data of bolted joints reported by Stelmokas (1995). Because of settlement effects, as the fastener gets pressed into the wood, stiffness increases from zero or close to zero in almost all cases. Attempts to fit the model to experimental data of bolts drilled at 1/16 inch oversize produced unsatisfactory results even after the slack was subtracted from the data (Figure 4.10). But even for general wood assemblies that do not exhibit slack, the BWBN model has some important limitations.

First, pinching in wood assemblies is strictly displacement controlled and not, as assumed in the BWBN model, a function of dissipated energy. This becomes clear when one considers a stabilized response, where the displacement amplitude does not change and energy is dissipated but pinching does not change.

Second, since the BWBN model is very dependent on dissipated energy, the model can only predict, with reasonable accuracy, the load-displacement function of systems that have similar energy demands as the one the model was calibrated to. The model cannot predict load–displacement functions for systems with higher energy demand than the one used to calibrate it, since the contribution of the hysteretic element that controls degradation can only decrease to zero, after which degradation is eliminated and the modeled solution approaches that of a linear spring-mass-damper system.

Third, versatility comes at a price. If experimental data are not noise-free, it is very difficult to identify the numerous parameters such that a satisfactory fit between model output and experimental data is achieved. Currently, there are no commercially available software packages that could assist with the fitting problem.

a) Test data

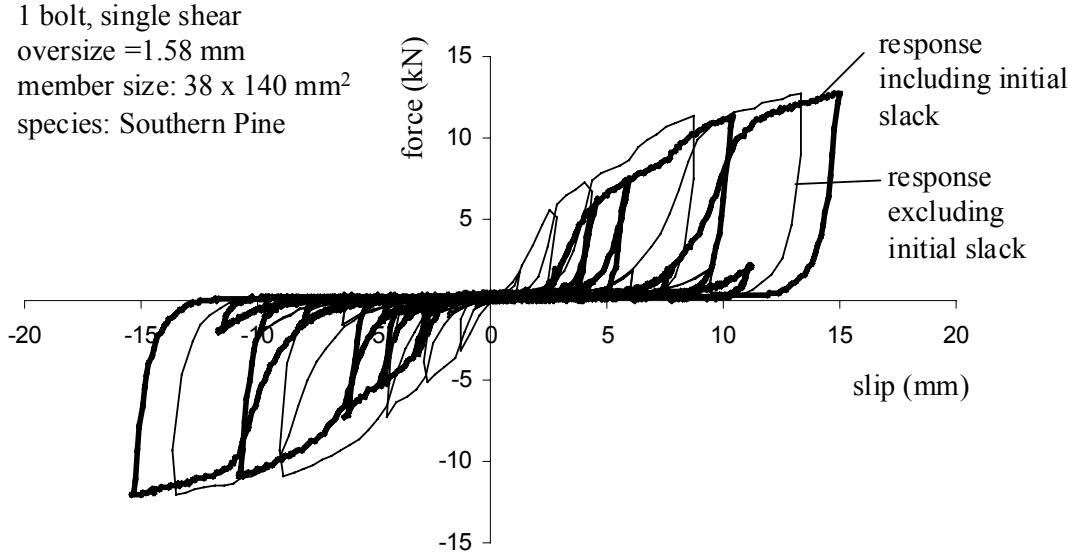

b) BWBN model solution to data excluding slack

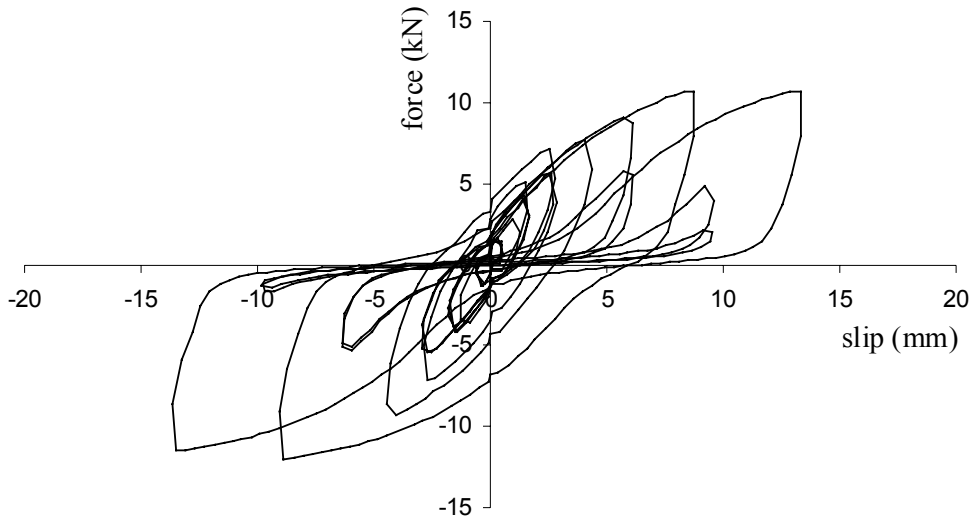

Figure 4.10: a) Load-slip plot of a single bolt in single shear subjected to reversed cyclic loading including slack and with slack subtracted from the data. b) Optimized fit of the BWBN model to the slack-free data carried out by CSIRO, Australia (Foliente 2001). Based on the way pinching is modeled, the BWBN model shows significant lack of fit for bolted joints especially around small displacements .